Catalysis Letters
https://doi.org/10.1007/s10562-019-02794-8

Synthesis of Fe_3O_4-DOPA-Cu Magnetically Separable Nanocatalyst: A Versatile and Robust Catalyst for an Array of Sustainable Multicomponent Reactions under Microwave Irradiation

Mitlesh Kumari[1] · Yachana Jain[1] · Priya Yadav[1] · Harshita Laddha[1] · Ragini Gupta[1,2]

Received: 27 February 2019 / Accepted: 21 April 2019

Abstract

Herein, we are reporting a facile route to synthesize magnetically separable copper loaded L-DOPA functionalized magnetite nanoparticles (Fe_3O_4-DOPA-CuNPs), which are well characterized by FT-IR, PXRD, SEM, EDAX, HRTEM, XPS, TGA and VSM techniques. This single catalyst exhibits excellent catalytic activity towards (i) synthesis of DHPMs via Biginelli reaction (ii) synthesis of imidazoles (iii) synthesis of 2-amino-4H-chromenes (iv) 1,2,3-triazole derivatives by 'Click reaction' under microwave irradiation (MWI). Interestingly it can be easily recovered and reused for subsequent cycles for above mentioned four important multicomponent reactions without any significant decrease in its catalytic activity.

Electronic supplementary material The online version of this article (https://doi.org/10.1007/s10562-019-02794-8) contains supplementary material, which is available to authorized users.

✉ Ragini Gupta
rgupta.chy@mnit.ac.in

[1] Department of Chemistry, Malaviya National Institute of Technology, Jaipur 302017, India

[2] Materials Research Centre, Malaviya National Institute of Technology, Jaipur 302017, India

Graphical Abstract

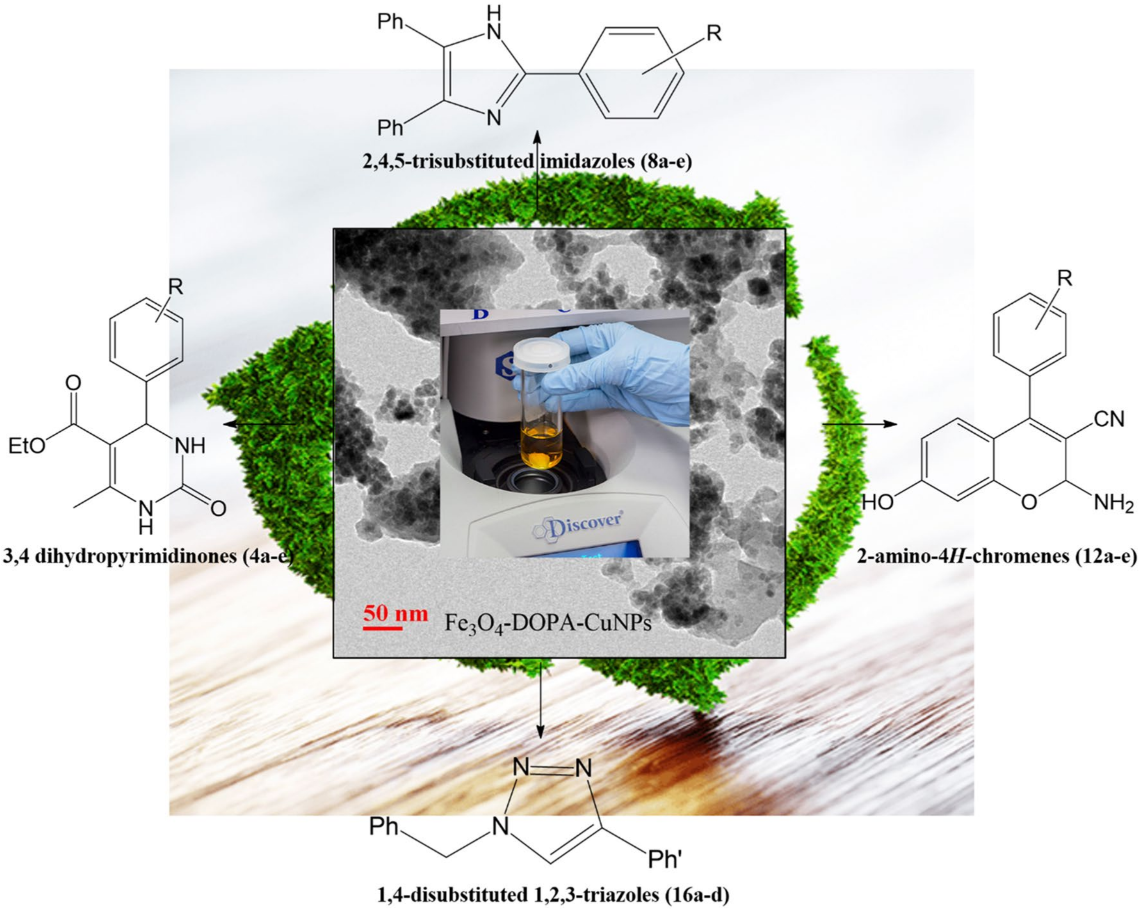

Keywords Magnetic nanocatalyst · Multicomponent reactions · L-DOPA · Fe$_3$O$_4$-DOPA-Cu

1 Introduction

MNPs have emerged as viable alternatives to conventional materials as robust, readily available, high surface area heterogeneous catalyst supports [1, 2]. Recently MNPs have found remarkable niche in diverse areas ranging from magnetic resonance imaging, magnetic targeting drug delivery to chemical catalysis, they increasingly serve as catalyst supports or are incorporated in the hybrid nanocomposite as sustainable catalyst for convenient separation and recycling [3–5]. Bare MNPs due to their inherent instability and hydrophobic nature results in big clusters over time in the absence of any surface coating which reduces their surface energy [6]. Therefore it needs to be minimized by surface immobilization of MNPs with biocompatible and organic and inorganic materials which protects them from being oxidized and provides them stability against damage during or after being used in organic transformations [7–9]. However most of the techniques require several steps to introduce functional groups to the magnetic surface and often involve the use of organosilica precursors as an organic shell to prepare a suitable support for incorporation of different transition metal ions [10–15]. Therefore, the preparation of modified MNPs via simple method and without using organoalkoxysiloxane compounds is highly desirable from both an environmental and economic point of view. The chemistry of copper is extremely rich because it can easily access Cu°, Cu^{I}, Cu^{II}, and Cu^{III} oxidation states allowing it to act through one electron or two electron process. This unique characteristic of Cu based nanocatalyst have made it suitable for many applications in nanotechnology, including catalytic organic transformations, electrocatalysis and photocatalysis. Because of the leaching effect and poor recyclability neat metal and oxide must be incorporated on some supports [16, 17]. In this respect, we introduce a simple and facile ultrasonication method for synthesis of highly water-dispersible magnetic nanoparticles, end-functionalized with non-toxic, biodegradable L-DOPA having amino and carboxyl groups as these are the most attractive functional groups, which are especially suitable for the immobilization of Cu nanoparticles. Multicomponent reactions (MCRs) whereby three or more reactants come together in a single vessel to create extremely ideal route for rapidly creating a library of diverse heterocyclic scaffolds. These reactions are highly atom economic since target compound obtained in one pot with much fewer steps containing all the atoms which are present in the substrates [18]. The combination of magnetic nanocatalyst and multicomponent reactions is an attractive research area and is an ideal blend for the development of sustainable methods in green synthetic chemistry [19]. In view of this we have investigated the catalytic activity of the synthesized Fe_3O_4-DOPA-Cu nanocatalyst towards four important multicomponent reactions: (i) 'Biginelli reaction' for the synthesis of DHPMs derivatives (ii) synthesis of 2,4,5 trisubstituted imidazole (iii) synthesis of 2-amino-4*H*- chromene and (iv) 'Click reaction' for the synthesis of 1,2,3 triazole derivatives.

Synthesis of DPHM and derivatives are important because of their wide range pharmaceutical and therapeutic applications such as calcium channel blockers, anti-inflammatory agents, antihypertensive, anti-tumor, adrenergic and neuropeptide antagonists [20–24] etc. Biginelli multicomponent reaction pathway is the most direct and elegant methodology for synthesis of DHPMs. Imidazoles have various biological applications as they are well known to anti-inflammatory, antiparasitic, antifungal, antiviral [25]. In addition used in photography as photosensitive compounds [26, 27], selective antagonists of the glucagon receptors and inhibitors of the IL-1 biosynthesis [28]. They are also the core structural skeleton in many important biological molecules like histidine, histamine, and biotin, as well as several drug moieties such as trifenagrel, eprosartan, and losartan [29–31]. The 4H-chromenes are major classes of natural oxygen-containing heterocyclic compounds, which are extensively found in ripe fruits and vegetables. Because of their different biological and pharmacological activities such as antioxidant, antileishmanial, antibacterial, antifungal, hypotensive, anticoagulant, antiviral, diuretic, antiallergenic, and antitumor activities [32–41], these compounds have occupied a key place in drug research. Synthesis of 1,4-disubstituted 1,2,3-triazoles by 'click reaction' has gained immense interest because it acts as scaffold for large number of biological active chemicals, pharmaceuticals, agrochemicals, drug molecules with significant anti-HIV activity, anti-microbial activity against Gram positive bacteria etc. [42–44]. Most of the synthetic methods are associated with one or more disadvantages such as using expensive reagents, prolonged reaction time, low yield of products, complex work-up procedures, formation of undesirable side products which can be resolved by microwave-assisted organic synthesis which is one of the most powerful and sustainable tools in synthetic chemistry due to its specific features including efficient atomic utilization, improved temperature regulation, reaction homogeneity, lesser reaction time and high product yield [45, 46]. Inspite of all these one more factor that is tedious recoverability of the catalyst particles hamper the sustainability and economics of the nanocatalytic strategy. Therefore to address all these issue, the development of such catalyst which will exhibit high catalytic activity along with easy recyclability and reusability for the synthesis of above described important MCRs is highly needed. So in continuation of our research endeavors towards the development of sustainable protocols and application of nanocatalyst [47, 48], herein we report on a highly efficient, versatile magnetically separable and recyclable Fe_3O_4- DOPA-Cu catalyst towards four important multicomponent reactions.

2 Experimental

2.1 Materials and Characterizations

All chemicals and solvents purchased are of analytical grade and used without further purification. Infrared spectra were collected on a Bruker Fourier transform infrared spectrophotometer (FTIR) (Alpha) with pressed KBr pellets and were recorded in the range of 4000-400 wave number (cm^{-1}). The visualization of surface morphology of MNPs was done by using a field- emission scanning electron microscope (FESEM; NOVA nano SEM) operated at a voltage 10 kV. Samples were prepared by putting a little amount of fine powdered nanoparticles on black carbon tape. Their TEM images were recorded with a Tecnai G^2 20 (FEI) S-Twin high-resolution transmission electron microscope (HRTEM) operating at 200 kV. Samples were prepared by drying the droplet of dispersed solution of MNPs on a 400 mesh carbon coated copper grid under 100 W table lamp. Powder X-ray diffraction (XRD) pattern of the sample was obtained with X-ray Diffractometer (Panalytical X Pert Pro) using Cu Kα radiation. X-ray photoelectron spectroscopy (XPS) measurements recorded in $ESCA^+$ omicron nanotechnology oxford instrument. Thermo gravimetric analysis (TGA) and differential thermal analysis (DTA) was performed on a Mettler thermal analyzer in an inert atmosphere at a heating rate of 10 °C/min. Melting points were determined in open glass capillaries using Gallenkamp melting point apparatus and are reported uncorrected. ^1H NMR were recorded on a Jeol ECS 400 MHz spectrophotometer using DMSO d_6 as a solvent. TMS was taken as an internal standard and chemical shifts are reported in δ ppm. Resonance multiplicities are described as s (singlet), d (doublet), t (triplet), q (quartet) and m (multiplet). Ultrasonic bath; Elma S 70 H with 37 kHz with an output frequency was used to carry out the sonochemical synthesis of nanoparticles and to carry out multicomponent reactions. CEM Discover Microwave was used to carry out all the multicomponent reactions. The purity of all the compounds was checked by TLC using silica gel as adsorbent and solvents of increasing polarity as mobile phase.

2.2 Preparation of Fe_3O_4- DOPA-Cu Nanocatalyst

The magnetite nanoparticles were synthesized by chemical co-precipitation method similar to previously reported method with slight modification [49]. In a 250 ml round bottom flask 16 mmol of $FeCl_3.6H_2O$ (4.32 g) and 8 mmol of $FeCl_2.4H_2O$ (1.59 g) were taken in 50 mL of deionised (DI) water and ultrasonicated for 15 min at room temperature (25 °C). Then slowly the temperature was raised to 60 °C and maintained for further 30 min. After that 50 mL of 1 M NaOH solution was added dropwise at the same temperature till the pH of the solution became 10-11. It was further sonicated for another 30 min. The resulting black dispersion was then allowed to remain undisturbed for one night and the desired nanoparticles were separated by using an external magnet then washed thoroughly with deionised water (5 × 100 mL) followed by acetone, (2 × 50 mL) and finally dried in a vacuum oven for 6 h at 60 °C. In order to graft L-DOPA over $Fe_3O_{4.}$ nanoparticles, the mixture of Fe_3O_4 (0.2 g) and L-DOPA (0.1 g) was ultrasonicated in deionized water (10 mL) at 80 °C for 2 h. Black precipitate of Fe_3O_4-DOPA was separated magnetically, washed with deionized water (3 × 20 mL) and dried under vacuum. Finally, for immobilization of Cu nanoparticles onto Fe_3O_4-DOPA, the aqueous solution of $CuCl_2 \cdot 2H_2O$ (0.01 g, 3 mL) was added into the dispersed solution of Fe_3O_4-DOPA (0.1 g) in $MeOH/H_2O$ (1:1, 10 mL), and the reaction mixture was ultrasonicated at room temperature for 0.5 h. Hydrazine hydrate was added till the pH of the solution became 9 followed by addition of $NaBH_4$ (0.01 g) into the reaction mixture which was further sonicated for 2 h. Fe_3O_4-DOPA-CuNPs so prepared was separated magnetically and washed successively with ethanol (2 × 20 mL) and water (2 × 20 mL). Finally, it was dried under vacuum at room temperature to get Fe_3O_4-DOPA-Cu nanoparticles as dark black powder.

2.3 General Procedure for the Synthesis of Dihydropyrimidinones via Biginelli Condensation Under Microwave Irradiation by Fe_3O_4-DOPA-Cu Nanocatalyst (4a-e)

25 mg of Fe_3O_4-DOPA-Cu nanocatalyst was added to a homogeneous mixture of aromatic aldehyde (1 mmol), ethylacetoacetate (1 mmol) urea (1.2 mmol) in a sealed pressure regulated 10 mL pressurized vial containing 5 ml of water/ethanol (1:1) with "snap-on" cap with a pressure sensor and a magnetic stirrer. The reaction tube was placed inside the cavity of a CEM Discover focused microwave synthesis system, operated at 80 °C, 100 Watts and 10–60 psi for 10-15 min. The reaction progress was monitored by thin layer chromatography (TLC, eluent: petroleum ether: ethyl acetate: 8: 2). After the completion of the reaction, the nano magnetite based catalyst was separated by using an external magnet and the reaction product was then poured into crushed ice. The obtained solid product was separated by simple filtration, washed with EtOH and dried and recrystallized from ethanol to afford pure product.

2.4 General Procedure for the Synthesis of 2,4,5-trisubstituted Imidazoles Under Microwave Irradiation by Fe_3O_4-DOPA-Cu Nanocatalyst (8a-e)

Fe_3O_4–DOPA–Cu (30 mg) as an efficient magnetic nanocatalyst was added to a mixture of benzil (1 mmol), aromatic aldehyde (1 mmol), NH_4OAc (4 mmol) in a sealed pressure regulated 10 mL pressurized vial with a pressure sensor and a magnetic stirrer containing 5 mL of ethanol. The reaction tube was placed inside the cavity of a CEM Discover focused microwave synthesis system, operated at 80 °C, 100 Watts and 10–60 psi for 15–18 min. After the TLC (eluent: petroleum ether:ethyl acetate:7:3) indicates the disappearance of starting materials, the reaction was cooled to room temperature. The resultant solid was dissolved in acetone and the magnetic nanocatalyst was separated using an external magnet. The mixture was concentrated on a rotary evaporator under reduced pressure and the solid product obtained was washed with water and recrystallized from acetone–water 9:1 (v/v) to afford the pure 2,4,5-trisubstituted imidazole derivatives.

2.5 General Procedure for the Synthesis of 2-amino-3-cyano-4H-Chromenes Under Microwave Irradiation by Fe_3O_4-DOPA-Cu Nanocatalyst

An equimolar mixture of resorcinol (1 mmol), malononitrile (1 mmol) and aromatic aldehyde (1 mmol) was placed in a sealed pressure regulated 10 mL pressurized vial containing ethanol (5 mL) and Fe_3O_4–PEG–Cu nanocatalyst (45 mg) with "snap-on" cap with a pressure sensor and a magnetic stirrer. The reaction tube was placed inside the cavity of a CEM Discover focused microwave synthesis system, operated at 60 °C, 100 Watts and 10–60 psi for 5–10 min. After completion of the reaction (TLC, eluent: petroleum ether:ethyl acetate:7:3), the mixture was poured into ice cold water. The resulting precipitate was filtered, dried and recrystallized from ethanol to afford pure 2-amino-4H-chromenes.

2.6 General procedure for synthesis of triazole via in situ generation of alkyl azide under microwave irradiation by Fe_3O_4-DOPA-Cu nanocatalyst

Alkyl halides (1.2 mmol), NaN_3 (1.5 mmol), alkyne (1.0 mmol) and Fe_3O_4–DOPA–Cu nanocatalyst (100 mg) in a sealed pressure regulation 10 mL pressurized vial containing 5 mL of water with "snap-on" cap with a pressure sensor and a magnetic stirrer. The reaction tube was placed inside the cavity of a CEM Discover focused microwave synthesis system, operated at 120 °C, 100 Watts and 10–60 psi for 10–12 min. After completion of the reaction, the catalyst was easily removed from reaction mixture using an external magnet. After separation of catalyst the solid product was filtered off or extracted with ethyl acetate and recrystallized or purified by column chromatography.

3 Results and Discussion

3.1 Characterization of the Fe_3O_4-DOPA-Cu nanocatalyst

In the present protocol, we have synthesized an efficient and magnetically recoverable catalyst, Fe_3O_4-DOPA-CuNPs and the process of its preparation has been schematically described in Scheme 1.

Firstly Fe_3O_4 nanoparticles were prepared by the co-precipitation method and were reacted with L-3,4 dihydroxyphenylalanine (L-DOPA) in water to yield the Fe_3O_4-DOPA and these obtained nanoparticles were further metallated with copper chloride in the presence of aqueous $NaBH_4$ solution to obtained the final copper decorated L-DOPA functionalized magnetic nanoparticles. The synthesized catalyst was characterized by various techniques such as FTIR, SEM–EDS, HRTEM, XPS, VSM, PXRD and TGA.

FTIR is one of the best technique to characterize the functionalization and modification of magnetite nanoparticles. The FTIR spectra of the magnetite, L-DOPA, Fe_3O_4-DOPA and Fe_3O_4-DOPA-Cu nanocomposites were recorded to

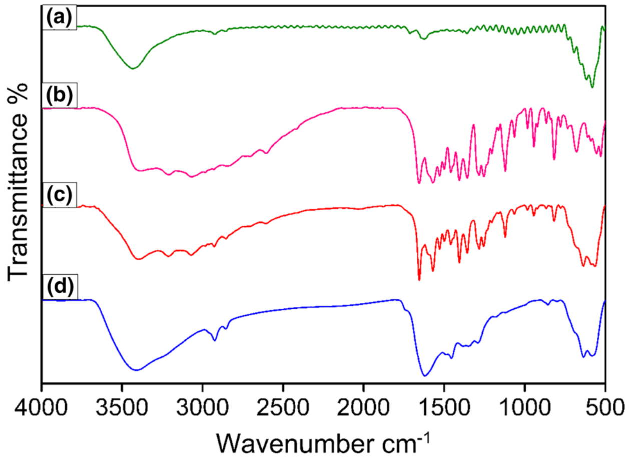

Fig. 1 FTIR spectra of **a** Fe_3O_4 **b** L-DOPA **c** Fe_3O_4-DOPA **d** Fe_3O_4-DOPA-CuNPs

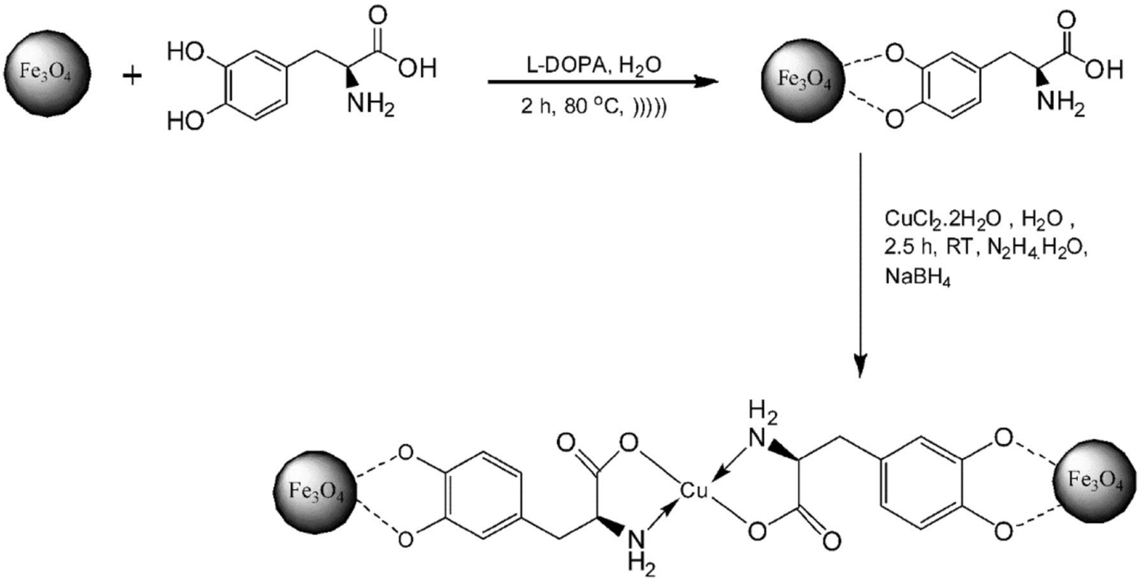

Scheme 1 Schematic representation of the synthesis of Fe_3O_4-DOPA-Cu nanocatalyst

confirm the modification of the magnetite surface with the L-DOPA and metal ion. (Figure 1a–d). The IR spectrum of Fe_3O_4 shows a broad band at 578 cm^{-1} due to the Fe–O stretching vibrational mode [50], Fig. 1a. The IR spectra of L-DOPA show a peak at 1656 cm^{-1} due to C = O stretching of carboxylic acid. The IR bands appearing at about 3408 cm^{-1} and 679 cm^{-1} correspond to the N–H stretching and bending vibration mode of L-DOPA as shown in Fig. 1b. Fe_3O_4-DOPA shows IR peak at 3402, 3206, 3071, 2919, 2840, 1651, 1465, 1405, 1274, 561 cm^{-1}. It has been observed that the stretching vibrational mode of the C–H of CH_2 group of L-DOPA appeared at 2919 cm^{-1} and 2840 cm^{-1} while the bending vibrational mode appeared at 1465 cm^{-1} [51]. Moreover, IR peaks at 1651 cm^{-1} and 1405 cm^{-1} could be ascribed to the carboxylate group of L-DOPA whereas the IR peak at 1274 cm^{-1} to the C-O stretching vibrational mode of the carboxylate group [50]. These results show that a large number of L-DOPA molecules are grafted over the Fe_3O_4 support. In terms of Fe_3O_4-DOPA-Cu (Fig. 1d), all the peaks become broaden and appears as band, and one of the noticeable change was a red shift of the band at 1651 cm^{-1} was observed (1651 cm^{-1} to 1617 cm^{-1}), which was probably characteristic of the asymmetrical fluctuations of the carbonyl group after interaction with the metal ion [52]. Overall, the IR results suggested that Cu was successfully immobilized onto the surface of Fe_3O_4-DOPA nanoparticles.

The crystalline structure of Fe_3O_4 and Fe_3O_4-DOPA-CuNPs were analyzed by powder X-ray diffraction (XRD). As displayed in Fig. 2a, b, according to the JCPDS card no. 19-0629, all the samples show diffraction peaks at around 30.4°, 35.5°, 43.3°, 53.4°, 57.2° and 62.8° which can be assigned to diffraction of Fe_3O_4 crystal with an inverse spinal structure from the (220), (311), (400), (422), (511), and (440) faces of the crystals, respectively. On assessment of the diffractograms of nanoparticles, the very distinguishable FCC peaks of the magnetite crystal were not changed, which means that these particles have phase stability, but there is a slight decrease in the intensity with broadening of the corresponding peak. The signals of Cu metal were not detected in XRD, indicating that Cu species is highly dispersed on ferrites.

Furthermore, the chemical composition of the Fe_3O_4-DOPA-Cu nanocomposite was determined by energy X-ray spectroscopy (SEM–EDX). The presence of C, N, O, Fe and copper centers in the nanocomposite was confirmed by elemental mapping images (Fig. 3). The result showed uniform distribution of Cu nanoparticles over the structure of the L-DOPA supported magnetite nanoparticles. The percentage of each element present in nanocatalyst were obtained from energy dispersive X-ray spectrum and the results obtained were in good agreement with the proposed catalyst composition (Fig. 4).

TEM image of the Fe_3O_4-DOPA-Cu nanocatalyst shows a somewhat spherical morphology, with some cubic partials, and an average size range of 8–20 nm with a mean particle size of 12 nm. The HRTEM image in Fig. 5b shows the characteristic lattice fringes of Fe_3O_4 nanoparticles with the d-spacing of 0.233 nm corresponds to the [311] plane of Fe_3O_4 [53]. Additional HRTEM image (Fig h) of Fe_3O_4-DOPA-Cu showed the lattice fringes with an interplanar spacing of approximately 0.216 nm corresponding to the [111] lattice plane of metallic Cu [54]. Figure 5i showed selected area electron diffraction pattern of the Fe_3O_4-DOPA-Cu nanocatalyst which revealed its polycrystalline nature.

In order to provide further evidence of the formation of Cu + 2 complex over the iron oxide core and to determine the oxidation state of copper, the XPS resolution spectroscopy have been investigated. For a better understanding of

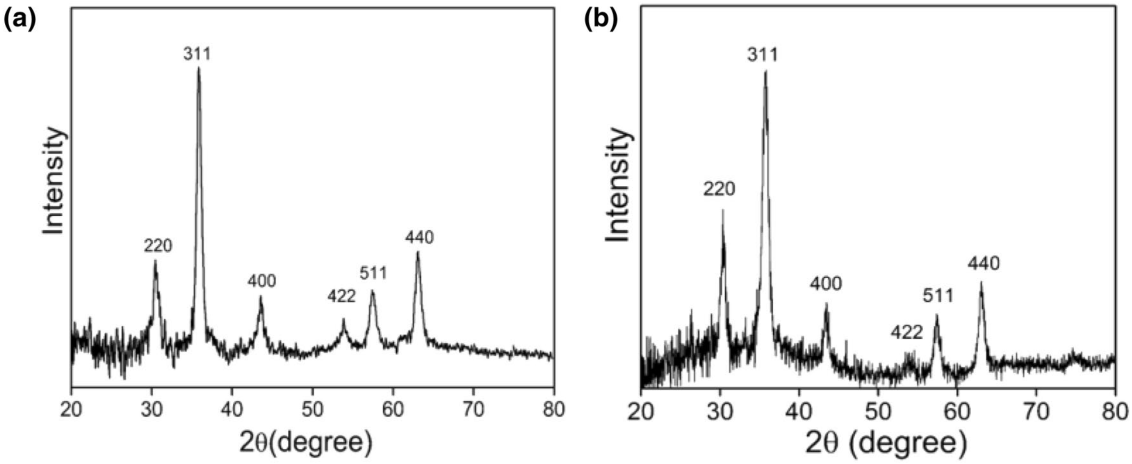

Fig. 2 XRD of **a** Fe_3O_4 **b** Fe_3O_4-DOPA-CuNPs

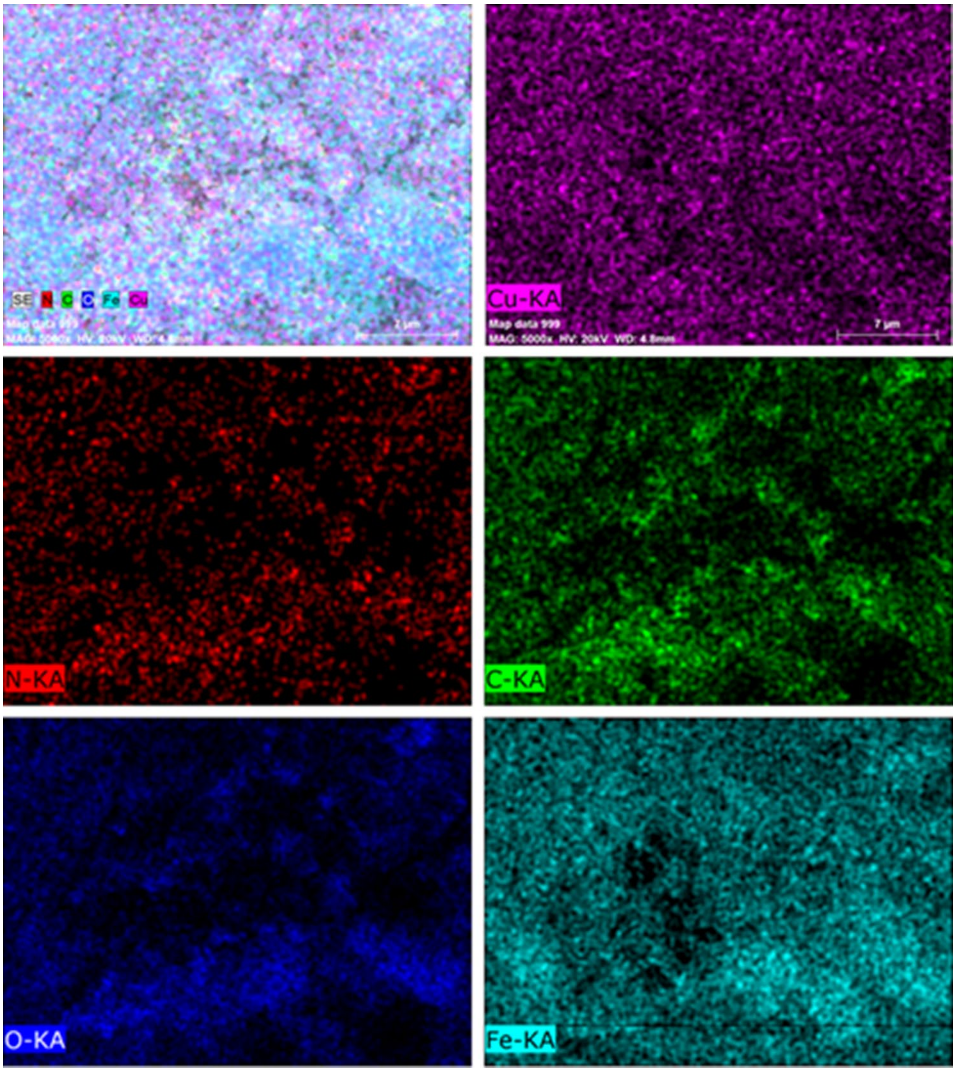

Fig. 3 EDS elemental mapping of the Fe_3O_4-DOPA-CuNPs

the oxidation state of copper, the binding energy obtained from the catalyst was compared with the Cu + 2 $2p_{3/2}$ and $2p_{1/2}$ peak positions. The binding energies of the main peaks were about 935.6 eV and 955.5 eV due to Cu $2p_{3/2}$ and $2p_{1/2}$, respectively [55]. Two other peaks were also obtained at 944.5 eV and 963.8 eV that attributed to the Cu $2p_{3/2}$ and $2p_{1/2}$ satellite peaks (Fig. 6b). Since all these lie within the given literature, it can be concluded that the oxidation state of copper in the catalyst is +2.

Another important parameter for the practical applications of nanoparticles is revealed from the VSM curve shown in Fig. 7a. The hysteresis loops of powdered material showed almost negligible magnetic hysteresis, with both the magnetization and demagnetization curves passing through the origin, which clearly indicates the supermagnetic nature of the materials. This also means that the magnetic material can only be aligned under an applied magnetic field, but it will not retain any residual magnetism upon removal of the field. Thus, Fe_3O_4-DOPA-Cu nanoparticles are sufficiently magnetic so that it can be easily separated from the reaction mixture by using an external magnet. The thermal stability of the synthesized nanocatalyst was also investigated by performing thermogravimetric analysis. The major weight loss was observed after 350 due to the decomposition of chemisorbed material i.e. L-DOPA. This confirms that thermal stability of the synthesized catalyst maintained at higher temperature.

3.2 Catalytic Activity

3.2.1 Catalytic Studies for the Synthesis of Dihydropyrimidinone (4a-e)

After characterization and demonstration of the structure and morphology of nanocatalyst, we examined its efficiency in the synthesis of 3,4-DHP derivatives under microwave irradiation. Initially, the reaction of benzaldehyde (1 mmol), ethyl acetoacetate (1 mmol) and urea (1.2 mmol) was taken

Fig. 4 EDS spectrum of Fe_3O_4-DOPA-CuNPs

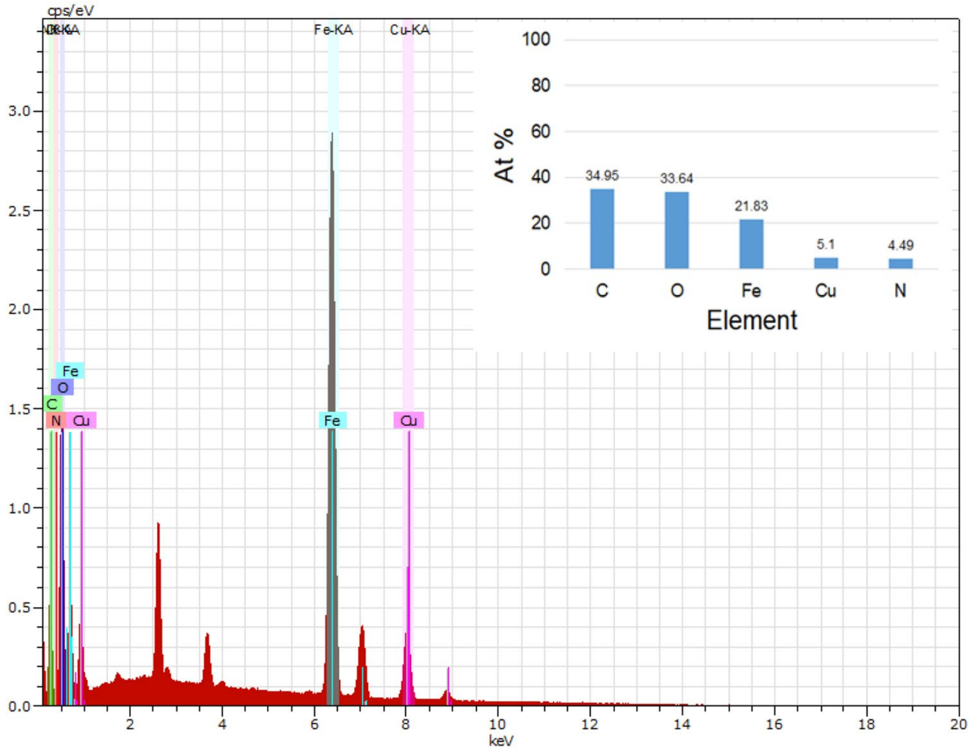

as a model reaction. The effect of solvent on reaction was examined along with catalyst amounts. Based on the results as shown in Fig. S2, 25 mg of Fe3O4-DOPA-Cu was considered as the optimum amount of catalyst and EtOH/H_2O as best suitable solvent. After the optimization of solvent and catalyst amount, we further examined the effects of the microwave power and temperature on the yield of the reaction. From obtained results depicted in Fig. S1, optimized power of microwave oven was 100 W at 80 °C. When the reaction has been carried out without using any catalyst it showed less yields in optimum time and after increasing time it gives quantitative yield. A comparative study with other synthetic method like conventional and ultrasonication has also been carried out, resulting best yield obtained by microwave irradiation in least reaction time (Fig. S3). Regarding to the obtained desired reaction conditions, we developed the present method for the reaction between benzaldehyde derivatives, ethyl acetoacetate and urea in the presence of optimum amount of catalyst. As shown in Table 1, products have high to excellent yields both in case of aldehydes bearing electron donating and electron withdrawing groups obtained in shorter reaction time. Products were characterized using physical and spectroscopic methods such as melting point, ^{1}HNMR technique. A proposed mechanism for the formation of dihydropyrimidines has been given in Scheme S1 based on the mechanism suggested by Kappe [56]. Initially the catalyst activated the carbonyl group of aldehyde followed by condensation by urea forming the intermediate A. The role of nanocatalyst is to increase the electrophilicity of carbonyl carbons of both aldehyde and ethylacetoacetate. The formation of enol structure favored by catalyst can be explained via HSAB theory. Here Cu^{+2} in the nanocatalyst act as harder acid due to the high charge density that is 6.2×10^2 nm^{-3} and the presence of low energy d-orbitals that can be used to hold the free electrons of the oxygen atom of ethylacetoacetate which can act as a base or nucleophile for chemical reactions. After that B intermediate was formed by nucleophilic addition of enol form of β-dicarbonyl to the intermediate A. Finally cyclization to the C intermediate subsequently proceeds by elimination of water to afford final product [57].

3.2.2 Catalytic Studies for the Synthesis of 2,4,5 Trisubstituted Imidazoles (8a-e)

To optimize the reaction conditions for the synthesis of 2,4,5 trisubstituted imidazoles, the reaction of benzaldehyde (1 mmol), benzil (1 mmol) and ammonium acetate (4 mmol) was used as a model reaction. Reactions were performed by varying microwave power and temperature, and the best optimum conditions obtained were 80 °C, 100 W. Further solvent optimization also carried out and the best suitable solvent observed was ethanol (Fig. S5 and S6). Optimization for catalyst loading has been also carried out revealed that the optimum amount of catalyst was 30 mg. The reaction showed less yields in optimum time when it has been

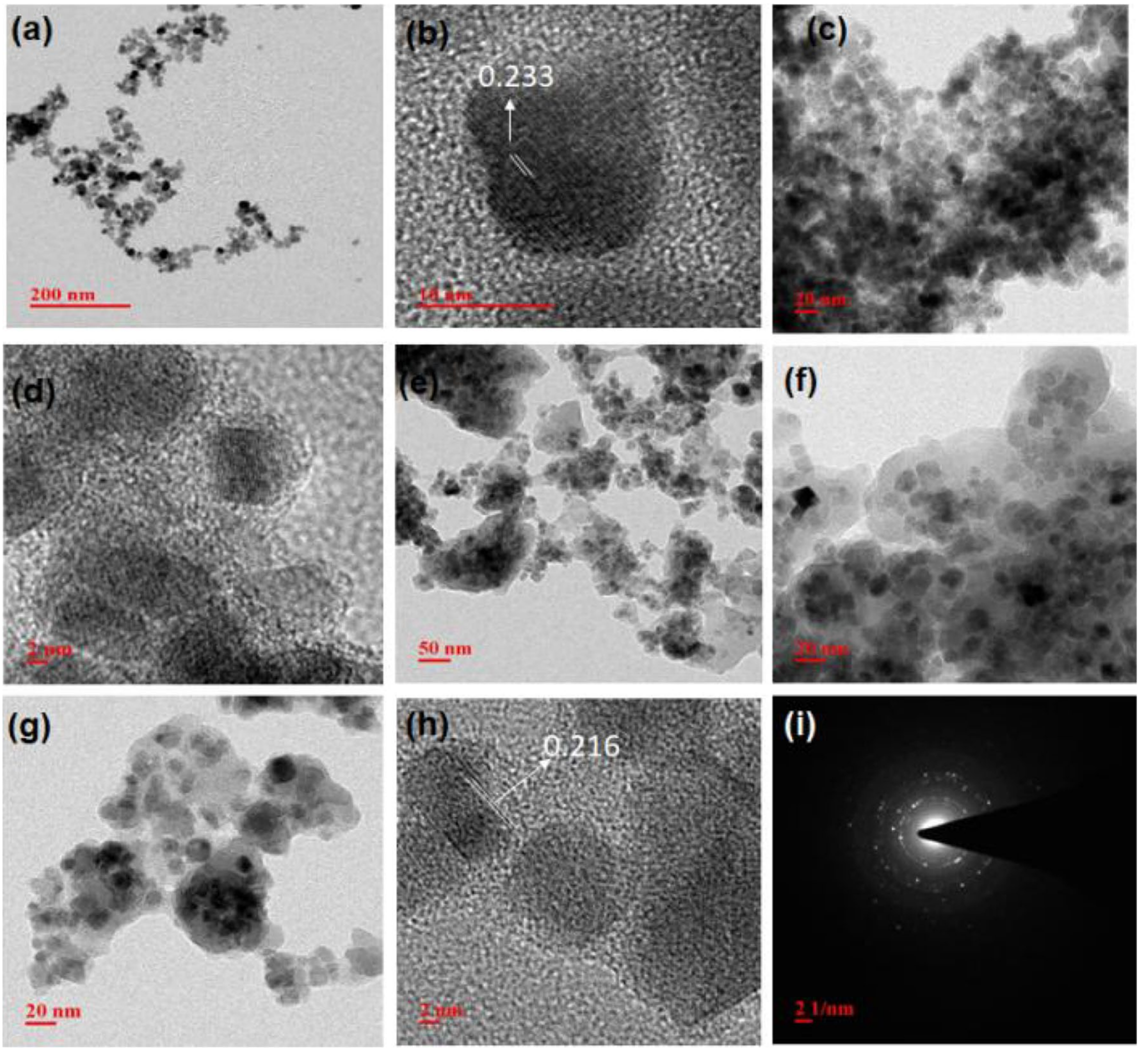

Fig. 5 **a** TEM image of Fe_3O_4 **b** HRTEM image of Fe_3O_4 **c** TEM image of Fe_3O_4 –DOPA **d** HRTEM image of Fe_3O_4 **e**, **f** and **g** TEM image of Fe_3O_4- DOPA-CuNPs **h** HRTEM image of Fe_3O_4- DOPA-CuNPs **i** SAED pattern of the of Fe_3O_4-DOPA-CuNPs

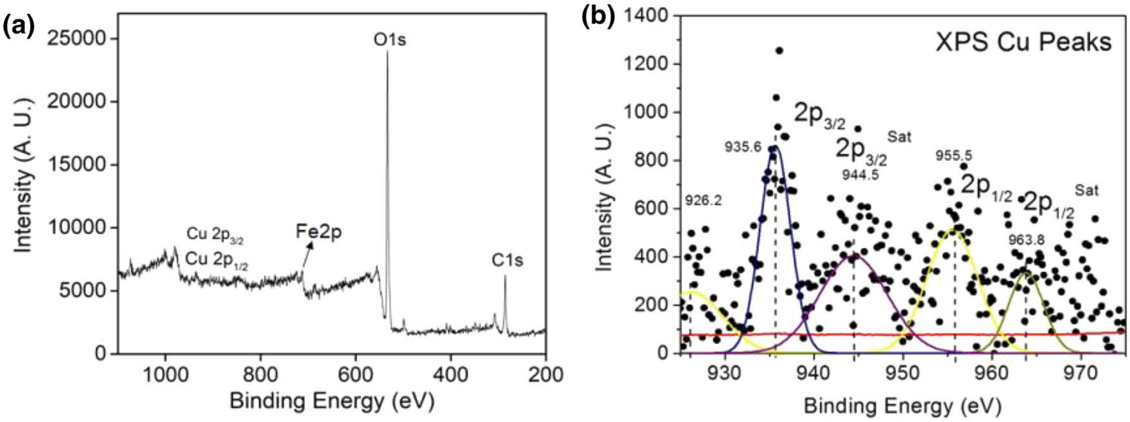

Fig. 6 X-ray photoelectron spectra of Fe_3O_4-DOPA-CuNPs showing Cu 2p3/2 and Cu 2p1/2 binding energies

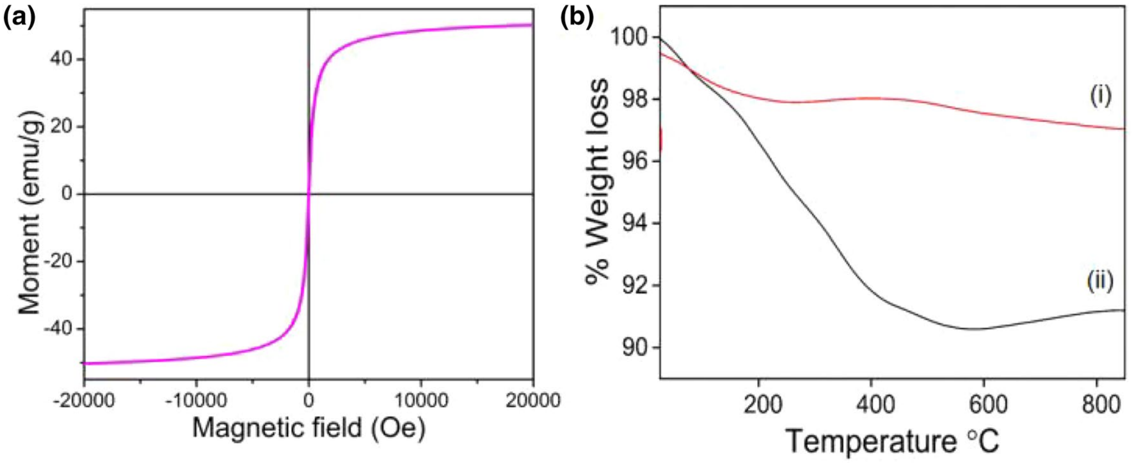

Fig. 7 **a** Room temperature magnetization curves of Fe_3O_4-DOPA-Cu **b** TGA of (i) Fe_3O_4 (ii) Fe_3O_4-DOPA-CuNPs

carried out without using any catalyst and after increasing time it gives quantitative yield. A comparative study has been carried out for various synthetic methods and microwave irradiation opted out as best method (Fig. S7). After optimizing the reaction conditions, in order to explore the scope and generality of this protocol, various aldehydes were used as substrate for the synthesis of 2,4,5 trisubstituted imidazoles. The results are shown in Table 2 and indicated that the reactions are equally facile with both electron withdrawing and electron donating groups present on the aromatic aldehydes, resulting in high yields of the corresponding imidazoles. Products were characterized using physical and spectroscopic methods such as melting point, ^{1}HNMR technique. The plausible mechanism for the synthesis of 2,4,5 trisubstituted imidazoles with the nanocatalyst shown in Scheme S2. Ammonium acetate is the source of ammonia molecule. At first the catalyst facilitates the formation of diamine intermediate (A) by increasing the electrophilicity of the carbonyl group of the aldehyde. Intermediate (A), undergo condensation with benzil to form intermediate (B) which further undergo condensation leading to intermediate (C) which rearranges via a [1, 5] sigmatropic shift to give the corresponding tri-substituted imidazole [58].

3.2.3 Catalytic Studies for Synthesis of 2-Amino-4H-Chromenes (12a-e)

Now to optimize the reaction conditions for the synthesis of 2-amino-4*H*-chromene, the reaction of benzaldehyde (1 mmol), malononitrile (1 mmol) and resorcinol (1 mmol) was used as a model reaction. Reactions were performed at different microwave power, temperatures, solvents, and catalyst loading resulting that the best condition were 60 °C, 100 W, 45 mg of the catalyst and ethanol as a solvent (Fig. S9, S10). The reaction has been carried out without using any catalyst also and it gives quantitative yield after increasing time but showed less yields in optimum time. For this reaction also a comparative study has been carried out for various synthetic methods and microwave irradiation opted out as best method (Fig. S11). After optimizing the reaction conditions, various aldehydes were used as substrate for the synthesis of 2-amino-4*H*-chromene. As shown in Table 3 aldehydes bearing either electron-withdrawing or electron donating groups showed equally well in the reaction and all 2-amino-4*H*-chromenes were prepared in high yields. Products were characterized using physical and spectroscopic methods such as melting point, ^{1}HNMR technique. The plausible reaction mechanism for the synthesis of 2-amino 4*H*-chromene derivatives in the presence of nanocatalyst is shown in Scheme S3. Firstly, catalyst binds with the oxygen of the carbonyl group makes the alpha hydrogen very acidic, thereby involving the Knoevenagel condensation reaction between aromatic aldehyde and malononitrile. In the second step, Knoevenagel product was reacted in a Michael addition with resorcinol to produce desired product after rearomatization and intramolecular cyclization with the help of nanocatalyst [59].

3.2.4 Catalytic Studies for Synthesis of 1,4 Disubstituted 1,2,3-Triazole (12a-d)

After preparing the catalyst, we examined its ability to promote the formation of the organic azide in situ, and subsequent 1,3-dipolar cycloaddition with the alkyne. We defined various parameters of analysis in order to optimize the reaction conditions. As can be seen from the Fig. S13 and S14 the influence of temperature, microwave power, solvent and catalyst loading were analysed. For the initial studies, we selected the reaction of benzyl bromide (1.2 mmol), sodium azide (1.5 mmol) and phenyl acetylene (1 mmol) as a model

Table 1 Fe_3O_4-DOPA-Cu catalyzed synthesis of 3,4 dihydropyrimidinones by Biginelli reaction

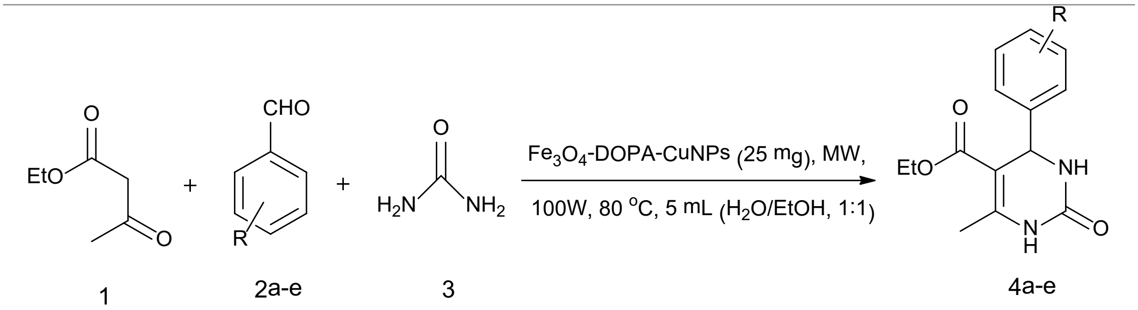

Entry	Product	Time (min)	[b]Yield %
4a	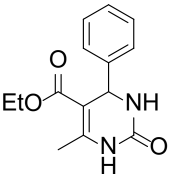	10	95
4b	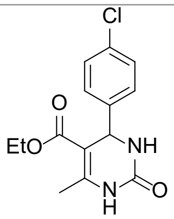	12	93
4c	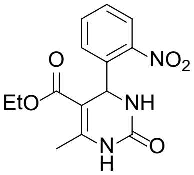	05	96
4d	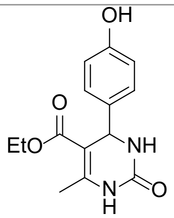	15	92
4e	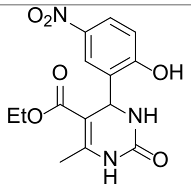	12	90

Reaction conditions: benzaldehyde (1 mmol), ethyl acetoacetate (1 mmol), urea (1.2 mmol) in the presence of 25 mg of Fe_3O_4-DOPA-CuNPs in 5 ml EtOH/H_2O, 100 W and 80 °C)

[a] Isolated yield

Table 2 Fe_3O_4-DOPA-Cu catalyzed synthesis of 2,4,5 trisubstituted imidazole

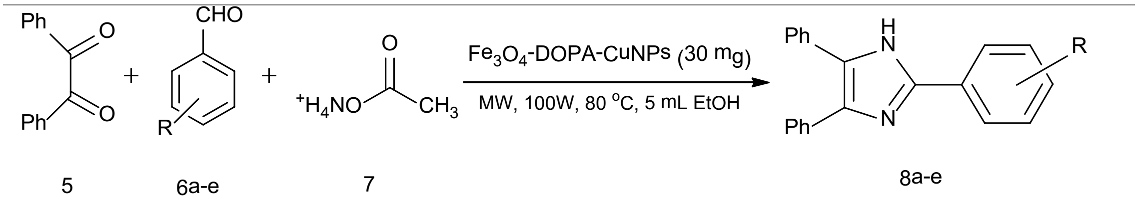

Entry	Product	Time (min)	Yield %
8a	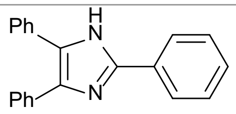	15	95
8b	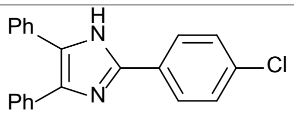	18	92
8c	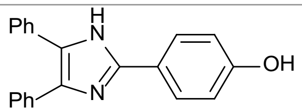	16	90
8d	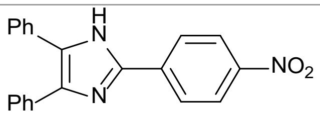	12	96
8e	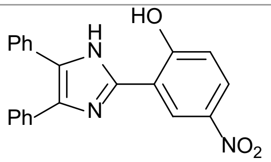	15	96

Reaction conditions: benzaldehyde (1 mmol), benzil (1 mmol), ammonium acetate (4 mmol) in the presence of 30 mg of Fe_3O_4-DOPA-CuNPs in 5 ml EtOH at 100 W and 80 °C)

[a] Isolated yield

reaction to yield the 1,2,3-triazole. It was observed that the optimum condition for the synthesis of triazole achieved were 100 W, 120 °C, 100 mg of the nanocatalyst and water as a solvent. In case of triazole synthesis, when the reaction was carried out without catalyst 1:1 of 1,4 and 1,5 cyclic adducts were obtained. The cycloaddition of alkyne and azide become region-selective and a very selective formation of 1,4 adduct in quantitative yield was observed with the help of Fe_3O_4–DOPA–Cu nanocatalyst. After independent optimization of the reaction conditions the same model reaction has been carried out under different synthetic methods like conventional heating, ultrasonication and microwave irradiation and results revealed that the best yield was obtained by microwave irradiation in less reaction time (Fig. S15). Further we extended these optimized conditions for different benzyl halides and terminal alkynes to check the versatility of the protocols and results obtained were mentioned in Table 4. Products were characterized using physical and spectroscopic methods such as melting point, ^{1}HNMR technique. Mechanism of copper catalysed synthesis of 1,2,3-triazoles has been recently been reviewed by Fokin who proposed a revisited mechanism whereby a σ-bound Cu(I)-acetylide bearing a π complexed copper atom reacts with an organoazide forming a bridging dicopper μ-acetylide intermediate [60–64]. Based upon their studies we proposed following mechanism for the formation of 1,2,3-triazoles (Scheme S4).

3.2.5 Recyclability and Leaching Aspect of the Fe_3O_4-DOPA-Cu Nanocatalyst

The reusability of the nanocatalyst was also examined and it is an important advantage of magnetic nanocatalyst that being magnetically separable from the reaction mixture, easily recovered by using an external magnet and can be reused for subsequent cycles. After every reaction they were washed

Table 3 Fe_3O_4-DOPA-Cu catalyzed synthesis of 2-amino-4*H*-chromenes

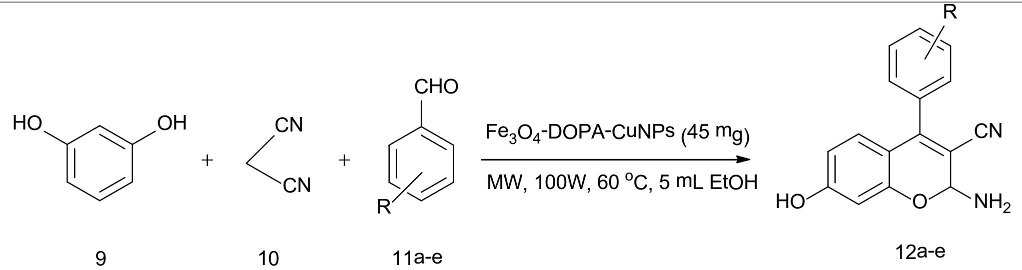

Entry	Product	Time (min)	[b]Yield %
12a	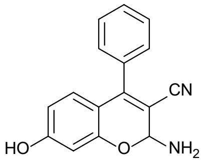	08	95
12b	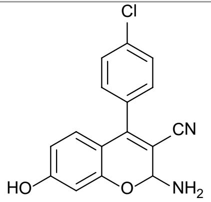	10	94
12c	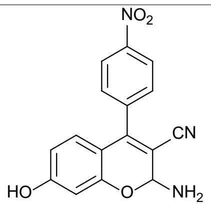	05	98
12d	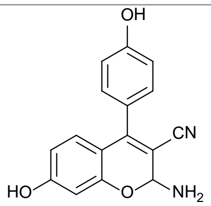	08	92
12e	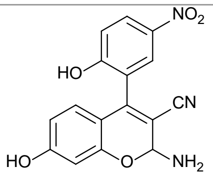	10	92

Reaction conditions: benzaldehyde (1 mmol), malononitrile (1 mmol), resorcinol (1 mmol) in the presence of 45 mg of Fe_3O_4-DOPA-CuNPs in 5 ml EtOH at 100 W and 60 °C)

[a] Isolated yield

with hot ethanol, air-dried and used directly for next round of reactions. The nanocatalyst was found to exhibit good catalytic activity for up to five reaction cycles for Biginelli reaction and triazole synthesis and up to six runs for imidazole and chromene synthesis.

The leaching aspect of any copper after recycling was examined by determining the metal content of reaction solution using AAS (atomic absorption spectroscopy) and sample digestions were carried out in a microwave oven at 500 W for 10 min with 5 mL aqua regia. It was found

Table 4 Fe_3O_4-DOPA-Cu catalyzed synthesis of 1,2,3- triazoles by Click reaction

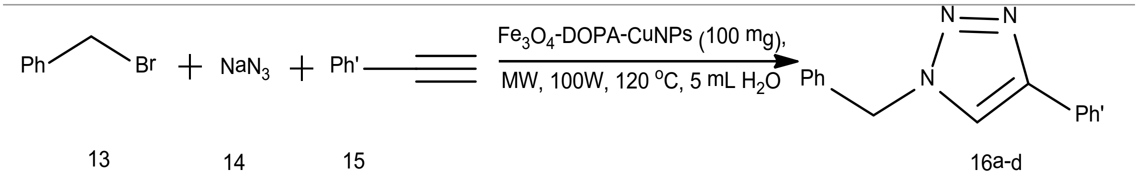

Entry	Product	Time (min)	^{b}Yield %
16a	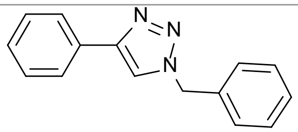	10	96
16b	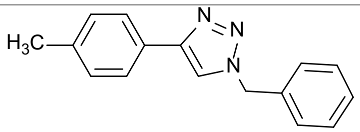	12	98
16c	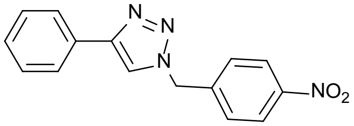	12	95
16d	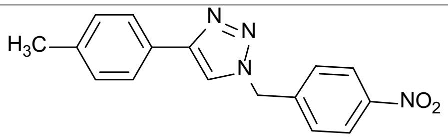	10	94

Reaction conditions: benzyl bromide (1.2 mmol), sodium azide (1.5 mmol), phenyl acetylene (1 mmol) in presence of 100 mg of Fe_3O_4-DOPA-CuNPs in 5 ml H_2O at 120 °C)

[a]Isolated yield

that the concentration of copper in the reused catalyst was reduced to 1.34 wt % for Biginelli reaction and 1.89 wt % for triazole synthesis after 5th run, 2.65 wt % for imidazole synthesis and 2.39 wt % for chromene synthesis after 6th run. The small amount of copper leaching might be due to some changes that occurred on the surface of the magnetic catalyst. Major weight loss of catalyst at high temperature and a small amount of leaching also proves that the catalyst is highly stable at high temperature also.

A comparative study of the reported methods in the literature to synthesize all the above described multicomponent reactions to show the efficiency of the catalyst. It is clear from the Tables S1-S4 given in the supplementary information that Fe_3O_4-DOPA-Cu is an efficient and environmentally benign nanocatalyst which could be used in the synthesis of an array of the above discussed important multicomponent reactions.

4 Conclusion

The synthesized catalyst (Fe_3O_4-DOPA-Cu) exhibits high catalytic activity towards (i) synthesis of DHPMs via Biginelli reaction (ii) synthesis of imidazoles (iii) synthesis of 2-amino-4H-chromenes (iv) 1,2,3-triazole derivatives by 'Click reaction' under microwave irradiation (MWI). The advantage of this catalyst are easy to prepare, inexpensive, and offers easy magnetic separation and reusability. Moreover the mild reaction conditions, operational simplicity, giving the desired product in high yields, easy work-up are the key advantages of this protocol. To the best of our knowledge, this is the first time one single catalyst is reported which shows its high activity for these four important multicomponent reactions and this fact makes it attractive.

Acknowledgements Authors are thankful to Materials Research Centre, MNIT Jaipur for providing spectral analysis facilities. M. Kumari acknowledge to Department of Science and technology (DST), India, for providing JRF under INSPIRE fellowship scheme (IF140506). One of the author Y. Jain is grateful to MNIT Jaipur for proving financial assistance. Other authors P. Yadav and H. Laddha are thankful to CSIR for providing JRF.

References

1. Nasir Baig RB, Varma RS (2012) Chem Commun 48:2582
2. Wang D, Astruc D (2014) Chem Rev 114:6949
3. Gawande MB, Monga Y, Zboril R, Sharma RK (2015) Coord Chem Rev 288:118
4. Shokouhimehr M, Hong K, Lee TH, Moon CW, Hong SP, Zhang K, Suh JM, Choi KS, Varma RS, Jang HW (2016) Green Chem 18:3184
5. Gawande MB, Goswami A, Felpin FX, Asefa T, Huang X, Silva R, Zou X, Varma RS (2016) Chem Rev 116:3722
6. Nasr-Esfahani M, Rafiee Z, Montazerozohori M, Kashi H (2016) RSC Adv 6:47298
7. Gawande MB, Branco PS, Varma RS (2013) Chem Soc Rev 42:3371
8. Shelke SN, Bankar SR, Mhaske GR, Kadam SS, Murade DK, Bhorkade SB, Rathi AK, Bundaleski N, Orlando MND, Zboril TR, Varma RS, Gawande MB (2014) ACS Sustain Chem Eng 2:1699
9. Abu-Dief AM, Fatah Abdel SMJ (2018) Basic Appl Sci 7:55–67
10. Li B, Gao L, Bian F, Yu W (2013) Tetrahedron Lett 2013(54):1063
11. Jin X, Zhang K, Sun J, Wang J, Dong Z, Li R (2012) Catal Commun 26:199
12. Esmaeilpour M, Sardarian AR, Javidi J (2012) Appl Catal A 445:359
13. Ucoski GM, Nunes FS, DeFreitas-Silva G, Idemori YM, Nakagaki S (2013) Appl Catal A 459:121
14. Sharma RK, Monga Y, Puri A, Gaba G (2013) Green Chem 15:2800
15. Yahyazadeh A, Gilandeh EA, Hashjin MA (2018) Catal Lett 148:1254
16. Allen SE, Walvoord RR, Salinas RP, Kozlowski MC (2013) Chem Rev 113:6234
17. Gawande MB, Goswami A, Felpin FX, Asefa T, Huang X, Silva R, Zou X, Varma RS (2016) Chem Rev 116:3722–3811
18. Cioc RC, Ruijter E, Orru RVA (2014) Green Chem 16:2958
19. Chen MN, Mo LP, Cui ZS (2019) Zhang ZH 15:27
20. Javidi J, Esmaeilpour M, Dodeji FN (2015) RSC Adv 5:308
21. Khosropour AR, Baltork IM, Ghorbankhani H (2006) Catal Commun 7:713
22. Alvim HGO, Lima TB, De-Oliveira AL, De-Oliveira HCB, Silva FM, Gozzo FC, Souza RY, Da Silva WA, Neto BAD (2014) J Org Chem 79:3383
23. Ghosh BK, Moitra D, Chandel M, Patra MK, Vadera SR, Ghosh NN (2017) Catal Lett 147:1061
24. Prakash GKS, Lau H, Panja C, Bychinskaya I, Ganesh SK, Zaro B, Mathew T, Olah GA (2014) Catal Lett 144:2012
25. Zheng H, Shi QY, Du K, Mei YJ, Zhang PF (2013) Catal Lett 143:118
26. Ma Gee DI, Bahramnejad M, Dabiri M (2013) Tetrahedron Lett 54:2591
27. Keivanloo A, Bakherad M, Imanifar E, Mirzaee M (2013) Appl Catal A 467:291
28. Gadekar LS, Mane SR, Katkar SS, Arbad BR, Lande MK (2009) Cent Eur J Chem 75:50
29. Koike H, Konse T, Sada T, Ikeda T, Hyogo A, Hinman D, Saito H, Yanagisawa H (2003) Annu Rep Sankyo Res Lab 55:1
30. Abrahams SL, Hazen RJ, Batson AG, Phillips AP (1989) J Pharmacol Exp Ther 249:359–365
31. Leister C, Wang Y, Zhao Z (2004) Lindsley CW Org Lett 6:1453
32. Ji SJ, Jiang ZQ, Lu J, Loh TP (2004) Synlett 5:0831
33. Zhang XY, Li YZ, Fan XS, Qu GR, Hu XY, Wang JJ (2006) Chin Chem Lett 17:150
34. Ivanciuc O, Ivanciuc T, Balaban AT (1998) Tetrahedron 54:9129
35. Huynh TH, Abrahamsen B, Madsen KK, Gonzalez-Franquesa A, Jensen AA, Bunch L (2012) Bioorgan Med Chem 20:6831–6839
36. Wang JL, Liu D, Zhang ZJ, Shan S, Han X, Srinivasula SM, Croce CM, Alnemri ES, Huang Z (2000) Proc Nat Acad Sci 97:7124
37. Manion MK (2003) Hockenbery D 2:104
38. Raj T, Bhatia RK, Sharma RK, Gupta V, Sharma D, Ishar MPS (2009) Eur J Med Chem 44:3209
39. Sabry NM, Mohamed HM, Khattab ESA, Motlaq SS, ElAgrody AM (2011) Eur J Med Chem 46:765
40. Vats P, Hadjimitova V, Yoncheva K, Kathuria A, Sharma A, Chand K, Duraisamy AJ, Sharma AK (2014) Med Chem Res 23:4907
41. Hajiashrai T, Karimi M, Heydari A, Tehrani AA (2017) Catal Lett 147:453
42. Sharghi H, Ebrahimpourmoghaddam S, Doroodmand MM, Purkhosrow A (2012) Asian J Org Chem 1:377
43. Naeimi H, Nejadshafiee V (2014) New J Chem 38:5429
44. Bhardwaj M, Jamwal B, Paul S (2016) Catal Lett 146:629
45. Gawande MB, Luque R, Zboril R (2014) Chem Cat Chem 6:3312
46. Gawande MB, Bonifa´cio VD, Luque R, Branco PS, Varma RS (2013) Chem Soc Rev 42:3371
47. Kumari M, Gupta R, Jain Y (2019) Synth Commun 49:529
48. Jain Y, Gupta R, Yadav P, Kumari M (2019) ACS Omega 4:3582
49. Saha S, Pal A, Kundu S, Basu S, Pal T (2010) Langmuir 26:2885
50. Niu J, Wang F, Zhu X, Zhao J, Ma J (2014) RSC Adv 4:37761
51. Sharma H, Bhardwaj M, Kour M, Paul S (2017) Mol Catal 435:58
52. Sharma H, Mahajan H, Jamwal B, Paul S (2018) Catal Comm 107:68
53. Rathore PS, Patidar R, Thakore S (2014) RSC Adv 4:41111
54. Hussain N, Gogoi P, Azhaganand VK, Shelke MV, Das MR (2015) Catal Sci Technol 5:1251
55. Mondal P, Sinha A, Salam N, Roy AS, Jana NR, Islam SM (2013) RSC Adv 3:5615
56. Kappe CO (2000) Acc Chem Res 33:879
57. Diarjani ES, Rajabi F, Yahyazadeh A, Santiago ARP, Luque R (2018) Materials 11:2458
58. Zarnegar Z, Safari J (2014) New J Chem 38:4555
59. Akocak S, Şen B, Lolak N, Şavk A, Koca M, Kuzu S, Şen F (2017) Nano-Struct Nano-Objects 11:25
60. Ayouchia HBE, Bahsis L, Anane H, Domingo LR, Stiriba SE (2018) RSC Adv 8:7670–7678
61. Rostovtsev VV, Green LG, Fokin VV, Sharpless KB (2002) Angew Chem Int Ed 41:2596–2599
62. Worrell B, Malik JA, Fokin VV (2013) Science 340:457
63. Liang L, Astruc D (2011) Coord Chem Rev 255:2933
64. Iacobucci C, Reale S, Gal JF, Angelis FD (2015) Angew Chem Int Ed 54:3065